

## Grating-based precision measurement system for five-dimensional measurement

LV Qiang<sup>1,2</sup>, WANG Wei<sup>1</sup>, LIU Zhao-wu<sup>1</sup>, SONG Ying<sup>1</sup>, JIANG Shan<sup>1</sup>, LIU Lin<sup>1,2</sup>,  
BAYANHESHIG<sup>1</sup>, LI Wen-hao<sup>1\*</sup>

(1. Changchun Institute of Optics, Fine Mechanics and Physics, Chinese Academy of Sciences,  
Changchun 130033, China;

2. University of Chinese Academy of Sciences, Beijing 100049, China)

\* Corresponding author, E-mail: liwh@ciomp.ac.cn

**Abstract:** To realize large range, high precision and multi-dimensional measurement with a relatively simple structure, a grating-based precise measurement system is designed for five-dimensional measurement including simultaneous measurement of displacement and angle. Based on symmetrical Littrow structure and heterodyne interference principle, two-dimensional displacement measurement along grating's vector direction and normal direction is realized by using one-dimensional diffraction grating with high groove density. What's more, the angle errors of pitch, yaw and roll of grating are measured by using high precision position sensitive detectors considering the angular variation between  $\pm 1^{\text{st}}$  order diffraction light and grating. Experimental results indicate that the proposed grating-based precision measurement system can achieve high precision and large range displacement measurement with resolution better than 4 nm. It can also realize high precision angle error measurement with resolution better than  $1''$ . Moreover, because the displacement measurement range is only limited by the size of grating, its measuring range is greatly increased. The grating-based precision measurement system is very important for high precision measurement of displacement and angle in the field of precision measurement.

**Key words:** grating; precision measurement; five-dimensional

## 五维自由度衍射光栅精密测量系统

吕强<sup>1,2</sup>, 王玮<sup>1</sup>, 刘兆武<sup>1</sup>, 宋莹<sup>1</sup>, 姜珊<sup>1</sup>, 刘林<sup>1,2</sup>, 巴音贺希格<sup>1</sup>, 李文昊<sup>1\*</sup>

(1. 中国科学院长春光学精密机械与物理研究所, 吉林 长春 130033;

2. 中国科学院大学, 北京 100049)

**摘要:** 为了在保证结构简单的前提下, 实现衍射光栅精密测量系统的大量程、高精度、多维度测量, 设计了能够同时测量

收稿日期: 2019-03-05; 修订日期: 2019-04-28

**基金项目:** 国家自然科学基金资助项目 (No. 61905245); 吉林省科技发展计划项目 (No. 20190303019SF, No. 20190103158JH); 广东省重点领域研发计划项目 (No. 2019B010144001)

Supported by National Natural Science Foundation of China (No. 61905245); Jilin Province Science & Technology Development Program Project (No. 20190303019SF, No. 20190103158JH); R & D projects in key areas of Guangdong Province (No. 2019B010144001)

位移和角度的五维自由度衍射光栅精密测量系统。基于利特罗对称式光路结构,采用高刻线密度的一维衍射光栅以及外差干涉原理实现了沿光栅矢量方向和光栅法线方向的二维位移测量;通过引入高精度的位置灵敏探测器,结合 $\pm 1$ 级衍射光与光栅之间的角度变化关系实现了对光栅俯仰、偏摆和滚转三个维度的角度误差测量。实验结果表明:该衍射光栅精密测量系统能够实现分辨力优于 4 nm 的二维位移测量以及分辨力优于 1" 的三维角度测量,其位移测量范围只受限于光栅的尺寸,量程大大增加。该衍射光栅精密测量系统在精密测量领域有重要意义。

**关键词:** 衍射光栅;精密测量;五维自由度

**中图分类号:** O439; TH741      **文献标识码:** A      **doi:** 10.3788/CO.20201301.0189

## 1 Introduction

With the advancement and development of science and technology, the modern processing and manufacturing field such as semiconductor manufacturing, precision machining, photolithography, *etc.* has put forward more and more stringent requirements for precision measurement technology<sup>[1-5]</sup>. The precision measurement technology that can take into account large range, high-precision and multi-dimensional measurement has become a powerful guarantee for the rapid development of modern processing and manufacturing industry. At this stage, precision measurement technology that can meet large range, high-precision and multi-dimensional measurement mainly includes laser interferometer and grating-based precision measurement system<sup>[6-8]</sup>. Grating-based precision measurement system is much less sensitive to environmental changes than the laser interferometer, and has greater advantages in environmental control and measurement costs than the laser interferometer<sup>[9-10]</sup>.

The methods of realizing multi-dimensional measurement with grating-based precision measurement system are mainly as follows: one-dimensional grating replaced by two-dimensional grating<sup>[11-12]</sup>; and the optical path structure by use of Michelson interferometer<sup>[13-14]</sup>. The manufacturing of two-dimensional gratings is more difficult than that of one-dimensional gratings, so the accuracy and size of the gratings are hard to guarantee. The optical path structure of Michelson interferometer can measure the displacement along the grating's normal direc-

tion. However, due to the limitation of the measurement principle, the range is limited by the size of the detector and the beam diameter. The measurement range is small, at most only a few millimeters, and the system is more complicated. Subsequently, the researchers adopted the Littrow optical path structure<sup>[15-17]</sup>, and two-dimensional displacement measurement along the grating's vector and normal directions can be realized by using one-dimensional grating. The measurement range of both dimensions is limited only by the size of the grating, which greatly increases the range of the system. The above are the ways to extend the dimension of displacement measurement of the grating-based precision measurement system. In 2009, two four-quadrant photodiode detectors were introduced by Liu *et al*<sup>[18]</sup>. That realized five-dimensional measurement. Due to the limitation of structure and principle, the displacement measurement range of this system is very small, only  $\pm 41 \mu\text{m}$  along the grating's normal direction in the experiment. In 2011, Gao *et al*<sup>[19]</sup> used a Position Sensitive Detector (PSD) which realized three-dimensional angular variations measurement of gratings. In 2013, the team proposed a grating-based precision measurement system for six-dimensional measurement in combination with the two-dimensional grating and Michelson interferometer structure<sup>[20]</sup>. Similarly, the displacement measurement range of the system is small due to the limitation of measurement principle and structure, the range is only  $1.2 \mu\text{m}$  along the grating's normal direction in the experiment. Moreover, the system is too complicated, which reduces the reliability and stability of the system.

The grating-based precision measurement system for five-dimensional measurement is proposed in the paper. This system introduces an angle measurement unit on the basis of Littrow-configured two-dimensional grating displacement measurement system to realize simultaneous measurement of displacement and angle. The system has a simple structure and a large displacement measurement range. The paper elaborates the principle of displacement and angle measurement and performance test has been conducted for the system through experiments. The experimental results indicate that the system can achieve high-precision, high-resolution, large range two-dimensional displacement, and high-precision, high-resolution three-dimensional angle measurement.

## 2 Principles

### 2.1 Structure of reading head

The reading head of the precision measurement system contains the displacement measurement unit and angle measurement unit. As shown in Fig. 1, the displacement measurement unit includes a beam splitter (BS), two polarization beam splitters (PBS<sub>1</sub>, PBS<sub>2</sub>), four quarter-wave plates (QW<sub>1</sub> ~ QW<sub>4</sub>), two attenuation plates (A<sub>1</sub>, A<sub>2</sub>), two plane mirrors (M<sub>1</sub>, M<sub>2</sub>), two partially reflecting mirrors (S<sub>1</sub>, S<sub>2</sub>) and two polarizers (P<sub>1</sub>, P<sub>2</sub>).

The laser emitted by the dual-frequency laser with a certain frequency difference and polarization directions perpendicular to each other is divided into the same two beams by the BS and then enters the left and right PBS, respectively. Take the light beam on the left as an example: after entering the PBS<sub>1</sub>, the laser is divided into transmissive light (P-polarized light) and reflective light (S-polarized light). P-polarized light becomes right-circularly polarized light through QW<sub>1</sub>, which is reflected by S<sub>1</sub> and incident on the grating at a Littrow angle. The diffracted light returns in the same way, and it becomes S-polarized light and is reflected by PBS<sub>1</sub> after

passing through QW<sub>1</sub>. It enters receiver R<sub>1</sub> through P<sub>1</sub>. After passing through QW<sub>2</sub>, M<sub>1</sub> and QW<sub>2</sub>, S-polarized light becomes P-polarized light, which finally enters the receiver R<sub>1</sub> through P<sub>1</sub> after transmission of polarization beam splitters.

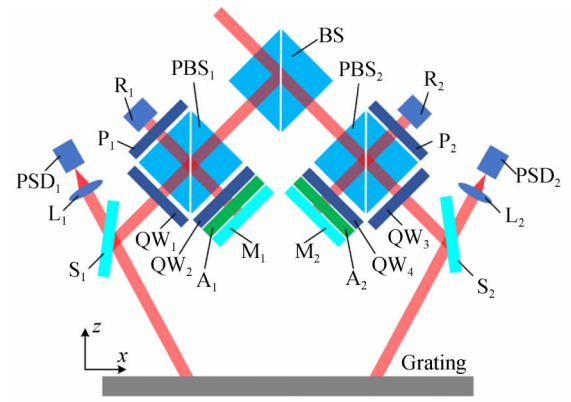


Fig. 1 Schematic diagram of grating-based precision measurement system

图1 衍射光栅精密测量系统结构示意图

In order to make the coherent light intensity close, an attenuation plate A<sub>1</sub> is added between QW<sub>2</sub> and M<sub>1</sub>. Because the transmission direction of P<sub>1</sub> and the vibration direction of the beam are 45°, the vibration directions of the two light beams passing through P<sub>1</sub> are parallel to each other and interference occurs. Similarly, the two light beams on the right side will also interfere into the receiver R<sub>2</sub>.

The angle measurement unit is composed of two identical convex lenses (L<sub>1</sub>, L<sub>2</sub>) and two position sensitive detectors (PSD<sub>1</sub>, PSD<sub>2</sub>). Part of the diffracted light is transmitted through partially reflecting mirrors (S<sub>1</sub>, S<sub>2</sub>) into the angle measurement unit. The PSD plane is placed at the focal point of the lens, and the laser is focused on the detector plane after passing through the lens. The detector detects the position of the focused spot in real time.

### 2.2 Principle of displacement measurement

When the grating moves, phase changes will be introduced by two interference signals as follows on the basis of the principle of grating Doppler frequency shift<sup>[21]</sup>:

$$\varphi_1 = \frac{4\pi\sin\theta}{\lambda}\Delta x + \frac{4\pi\cos\theta}{\lambda}\Delta z, \quad (1)$$

$$\varphi_2 = -\frac{4\pi\sin\theta}{\lambda}\Delta x + \frac{4\pi\cos\theta}{\lambda}\Delta z, \quad (2)$$

where,  $\varphi_1$  and  $\varphi_2$  represent the phase changes introduced by the left and right measurement beams due to the grating movement,  $\theta$  is the Littrow angle of the laser incident on the grating,  $\lambda$  is the wavelength of the laser,  $\Delta x$  is the displacement along the grating's vector direction ( $x$  direction) and  $\Delta z$  is the displacement along the grating's normal direction ( $z$  direction).

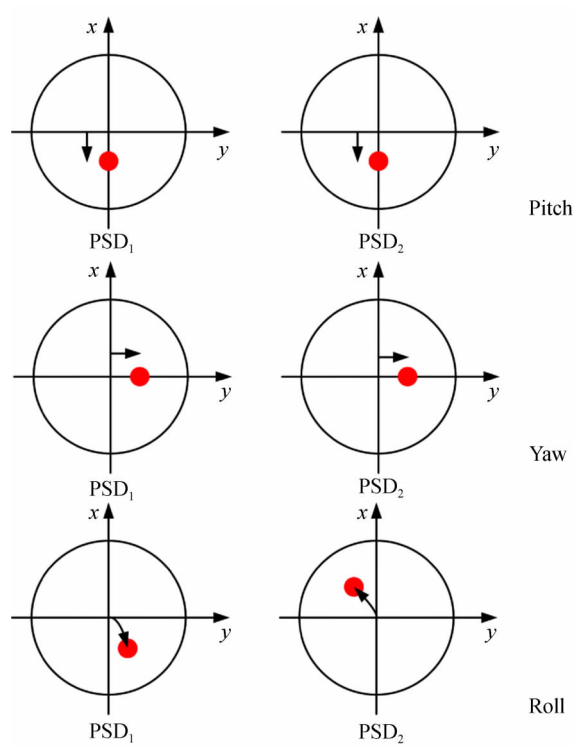


Fig. 2 Schematic diagram of the relationship between spot position and the rotation angle of the grating

图 2 光斑位置与光栅旋转角度关系的示意图

According to eq. (1), eq. (2) and Littrow-configured grating equation  $2d\sin\theta = m\lambda$  ( $m = 1, 2, 3 \dots$ ), the grating displacements in these two directions can be calculated as follows:

$$\Delta x = \frac{d}{4\pi m}(\varphi_1 - \varphi_2), \quad (3)$$

$$\Delta z = (\varphi_1 + \varphi_2) \frac{d}{4\pi m \cot\theta}, \quad (4)$$

where,  $d$  represents the grating period.

## 2.3 Principle of angle measurement

When the grating has an angular error, the diffracted light will be yawed due to the change of the incident angle, causing the spot position on the PSD to change. According to the matrix analysis method of geometric optics<sup>[22]</sup>, we can know the relationship between the rotation of the grating and the spot position on the PSD, as shown in Fig. 2.

When there is a change in the pitch angle of the grating, the two diffracted beams will move along the grating groove direction at the same time, so the two spots will move by the distance  $x_1$  and  $x_2$  respectively in the same direction of the  $x$  axis of the PSD, and  $x_1 = x_2$ ; when the grating has a yaw error, the two diffracted beams will move along the grating's vector direction at the same time, so the two spots will move by the distance  $y_1$  and  $y_2$  in the same direction of the  $y$  axis of the PSD, and  $y_1 = y_2$ ; when the grating has a roll error, the two spots will move  $z_1$  and  $z_2$  in opposite directions in the first/third quadrant or second/fourth quadrant of PSD plane coordinate system, respectively, and  $|z_1| = |z_2|$ . Therefore, the following pitch angle, yaw angle and roll angle of the grating can be obtained from the geometric relationship:

$$\theta_x = \frac{x_1 + x_2}{4f}, \quad (5)$$

$$\theta_y = \frac{y_1 + y_2}{4f}, \quad (6)$$

$$\theta_z = \frac{z_1 - z_2}{4f} = \frac{\sqrt{(x_1^2 + y_1^2)} - \sqrt{(x_2^2 + y_2^2)}}{4f}. \quad (7)$$

## 3 Experiments and Testing

In order to verify the performance of the precision measurement system, an experimental platform was set up and a series of tests were performed. The

tests include angle measurement test and displacement measurement test. Fig. 3 is a schematic diagram of experimental device for angle measurement. The laser emitted by a He-Ne dual-frequency laser with a wavelength of 632.8 nm is incident on the reading head of the grating-based precision measurement system. Two light beams emitted by the reading head enter into the reflective grating with a period of 555 nm and a size of 50 mm × 25 mm × 6 mm at a Littrow angle. Part of the two diffracted light passes through the partially reflecting mirrors and is incident on a lens with a focal length of 400 mm, and is converged by the lens to two PSDs at the focal plane. PSD uses OBP-U-9H produced by Newport. In the test, the accuracy of the angle measurement was checked through a photoelectric autocollimator DA20 (with an accuracy of 0.02") produced by Taylor Hobson. The grating and two plane mirrors are fixed on a rotating platform which is composed of three Newport angular platforms, and the three platforms are equipped with the Newport's miniature piezoelectric linear actuators.

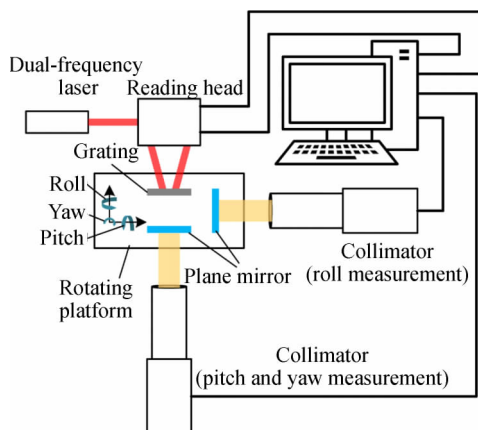


Fig. 3 Diagram of experimental device for angle measurement

图3 角度测试实验装置图

Fig. 4 is a schematic diagram of experimental device for displacement measurement. Different from the angle measurement test, the displacement measurement results of the dual-frequency laser interfer-

ometer and the grating-based precision measurement system are compared. Newport's precision one-dimensional linear displacement platform xml210-s is used to replace the rotary platform.

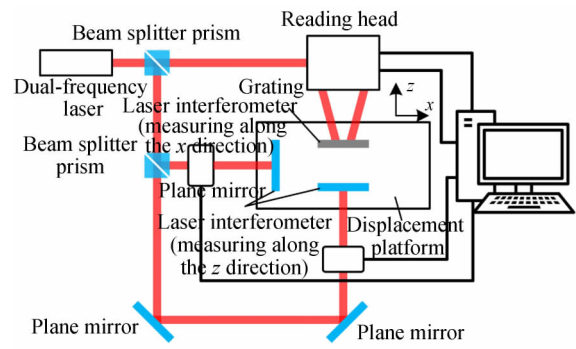


Fig. 4 Diagram of experimental device for displacement measurement

图4 位移测试实验装置图

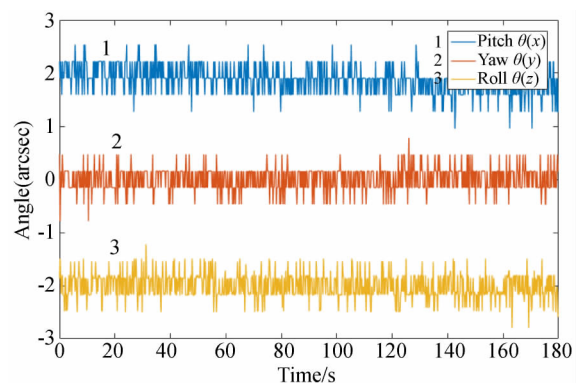


Fig. 5 Rotation angle measurement results in three directions by proposed system at rest

图5 静止时衍射光栅精密测量系统对3个方向的测量结果

Fig. 5 shows rotation angle measurement results in three directions by the grating-based precision measurement system at rest. For easy observation, the measurement results of the pitch angle and roll angle are translated by 2" along the positive and negative directions of the Y axis, respectively. It can be seen from the figure that the measurement results of the three angles are all stable, and the vibration amplitude is small. The vibration at high frequencies is mainly caused by electronic noise. The  $3\sigma$  values

are  $0.77''$ ,  $0.68''$  and  $0.72''$ , which can show that the system can also realize high precision angle error measurement with resolution better than  $1''$ .

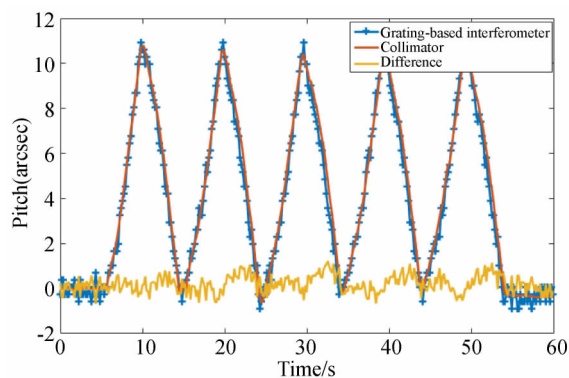


Fig. 6 Measurement results of pitch angle for  $10''$  change  
图 6 俯仰角变化  $10''$  的测量结果

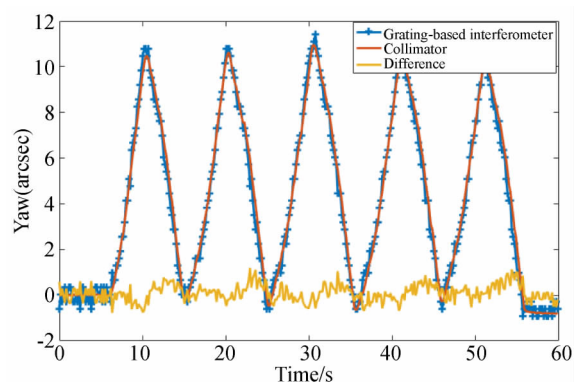


Fig. 7 Measurement results of yaw angle for  $10''$  change  
图 7 偏摆角变化  $10''$  的测量结果

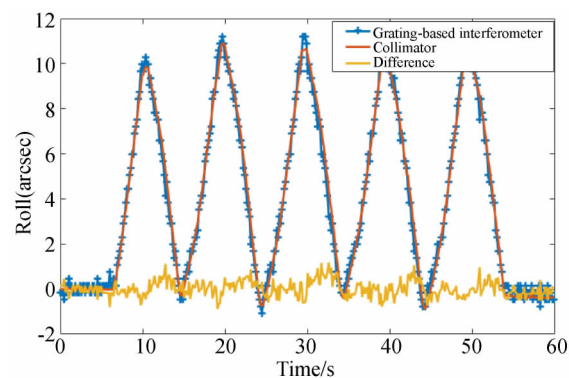


Fig. 8 Measurement results of roll angle for  $10''$  change  
图 8 滚转角变化  $10''$  的测量结果

The miniature piezoelectric linear actuator is adjusted so that the minimum displacement is 5-step, and then makes it do back and forth movement. As the displacement measurement unit will not work when the angle changes greatly, the angle change range shall be controlled within  $10''$ . The measurement results of pitch angle, yaw angle and roll angle of grating-based precision measurement system and photoelectric autocollimator are shown in Figs. 6 ~ 8 (Color online). In the three figures, the solid blue line with the symbol of "+" represents the angle measurement results of the grating-based precision measurement system, the solid red line represents the measurement results of the photoelectric autocollimator, and the solid yellow line represents the difference between the two measurement results. It can be clearly seen from the figures that the measurement results of the rotation angles in the three directions by the two systems are consistent. The difference of the measurement results fluctuates around 0, and the  $3\sigma$  values are  $1.18''$ ,  $1.11''$  and  $1.07''$ , respectively. The difference is mainly caused by electronic noise, environmental vibration and uncleaned cosine errors. The experimental results prove that the grating-based precision measurement system can achieve high-precision angle measurement in the range of  $10''$  and has good measurement repeatability.

Figs. 9-11 (Color online) shows the measurement results of pitch angle, yaw angle and roll angle, respectively. The miniature piezoelectric linear actuator is adjusted so that the minimum displacement is 25-step, and then compares it with the measurement results of the photoelectric autocollimator. In the figures, the solid red line with the symbol of "+" represents the measurement results of the grating-based precision measurement system, the solid blue line represents the measurement results of the photoelectric autocollimator, and the solid green line represents the difference between the two measurement results. It can be seen from the figures that



the angle change is less than  $1''$  when the piezoelectric actuator move every 25 steps. The measurement results are not symmetrical due to the influence of factors such as hysteresis error, but both systems can detect the angle change, and the measurement results are consistent. The difference of the measurement results fluctuates around 0, and the  $3\sigma$  values are  $0.83''$ ,  $0.74''$  and  $0.78''$ , respectively. The experimental results prove that angle measurement resolution of the grating-based precision measurement system is better than  $1''$ , and the system can achieve high-precision high-resolution angle measurement and meet the needs of precision machining.

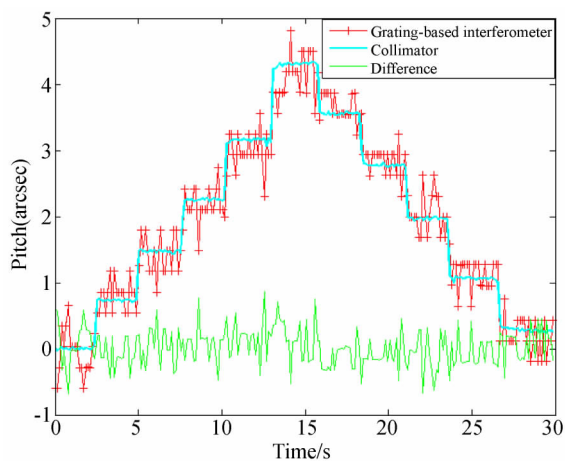


Fig. 9 Measurement results of pitch angle for  $1''$  change

图9 俯仰角变化  $1''$  的测量结果

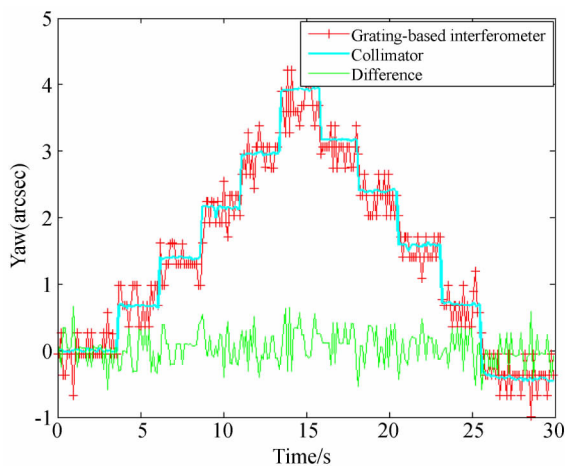


Fig. 10 Measurement results of yaw angle for  $1''$  change

图10 偏摆角变化  $1''$  的测量结果

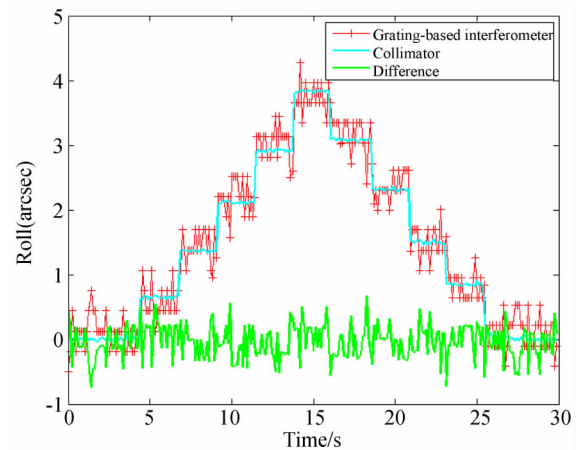


Fig. 11 Measurement results of roll angle for  $1''$  change

图11 滚转角变化  $1''$  的测量结果

Figs. 12-15 (Color online) show the displacement measurement results where Fig. 12 and Fig. 13 are the displacement measurement results for 5 mm in the  $x$  direction and the  $z$  direction respectively. In the figures, the solid red line with the symbol of "+" represents the displacement measurement results of the grating-based precision measurement system, the solid blue line represents the measurement results of the dual-frequency interferometer, and the solid green line represents the difference between the two measurement results. It can be seen from Fig. 12 that the measurement results for 5 mm displacement in  $x$  direction of the grating-based precision measurement system and dual-frequency interferometer are consistent.  $3\sigma$  value of the measurement results difference is 30.62 nm. It can be seen from the small figure that a low-frequency vibration between the two measurement results is mainly caused by the surface shape of the grating, the groove error and environmental fluctuations. Because the poor grating surface shape and groove will result in phase differences to the left and right parts of the displacement measurement unit of the grating-based precision measurement system, as a result, there is an error in the measurement results. It can be seen from Fig. 15 that measurement results of the two systems for 5 mm displacement in  $z$  direction are consistent, and  $3\sigma$  value of the measurement results differ-

ence is 20.44 nm. Similarly, low-frequency vibration is mainly caused by the surface shape error of the grating, the groove error and the change of the surrounding environment. Due to the use of the Littrow structure, the displacement measurement range of the system in both directions is limited only by the grating size. Moreover, the one-dimensional grating can be made very long, so the system can easily realize the displacement measurement in the millimeter range. As the grating size increases, the range will increase, which is much larger than the displacement measurement range of current multi-dimensional measurement system based on Michelson structure.

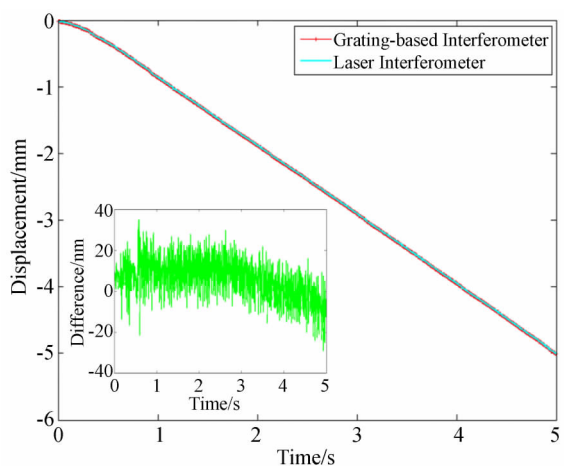


Fig. 12 Measurement results for 5 mm displacement in  $x$  direction

图 12  $x$  方向 5 mm 位移测量结果

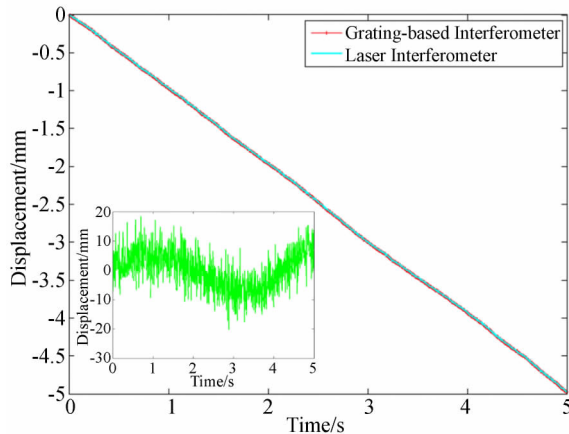


Fig. 13 Measurement results for 5 mm displacement in  $z$  direction

图 13  $z$  方向 5 mm 位移测量结果

Fig. 14 and Fig. 15 show the displacement measurement results in  $x$  direction and  $z$  direction, respectively. In the figures, the solid red line with the symbol of " + " represents the displacement measurement results of the grating-based precision measurement system, the solid blue line represents the measurement results of the dual-frequency laser interferometer, and the solid green line represents the difference between the two measurement results. It can be seen from the above two figures that the grating-based precision measurement system can resolve displacement changes less than 4 nm. The measurement results of the grating-based precision measurement system and dual-frequency interferometer are consistent, and  $3\sigma$  value of the measurement results difference is 1.67 nm and 2.65 nm, respectively. It can be seen from eq. (9) that the displacement measurement value in  $z$  direction is not only related to the grating period, but also to the incident angle. Therefore, it is more affected by the environment than that in  $x$  direction, the displacement curve at rest is more volatile and the error is larger than that in  $x$  direction.

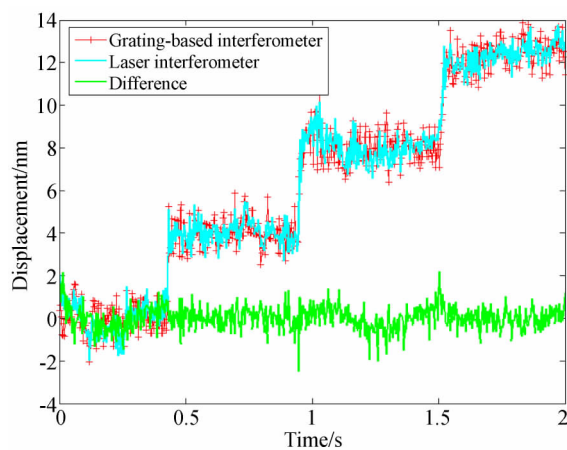


Fig. 14 Measurement results for 4 nm displacement in  $x$  direction

图 14  $x$  方向 4 nm 位移测量结果



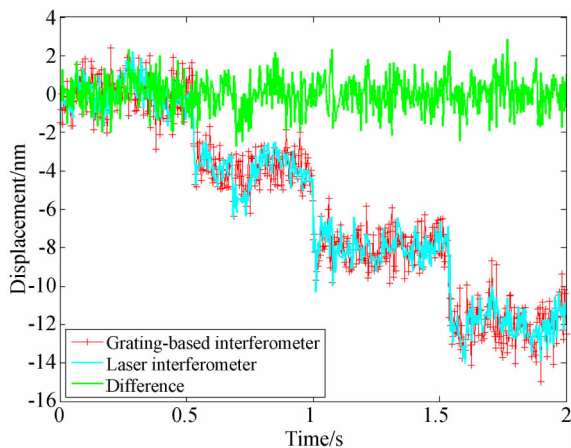


Fig. 15 Measurement results for 4 nm displacement in  $z$  direction

图 15  $z$  方向 4 nm 位移测量结果

## 4 Conclusions

In this paper, grating-based precision measurement system for five-dimensional measurement that can simultaneously realize two-dimensional displacement measurement and three-dimensional angle measurement is proposed. The system solves the problems of the complex structure and small range of the current grating-based multi-dimensional measurement system.

It has the advantages of simple structure, large displacement range, high accuracy and high resolution. The basic structure and measurement principle of the system are elaborated, and a series of tests are performed for angle measurement and displacement measurement. The experimental results show that three-dimensional angle measurement with the resolution of the grating-based precision measurement system is better than  $1''$ . For an angle change of  $10''$ , the  $3\sigma$  value of the difference from the measurement results of the photoelectric autocollimator is about  $1''$ ; for an angle change of  $1''$ , the  $3\sigma$  value of the difference from the measurement results of the photoelectric autocollimator is about  $0.8''$ . The resolution of two-dimensional displacement measurement is better than 4 nm. For the 4 nm displacement change, the  $3\sigma$  value of the difference from measurement results of the dual-frequency laser interferometer is about 2 nm. For the 5 mm displacement change, the  $3\sigma$  value is better than 31 nm. The system with simple structure and strong practicability is very important to the field of precision and ultra-precision machining.

——中文对照版——

## 1 引言

随着科技的进步与发展,半导体制造、精密机械加工、光刻等<sup>[1-5]</sup>现代加工与制造领域对精密测量技术提出了越来越严苛的要求,能够兼顾大量程、高精度、多维度测量的精密测量技术已成为现代加工制造业迅速发展的有力保障。现阶段可以满足大量程、高分辨力、高精度、多维度测量的精密测量技术主要有激光干涉仪和光栅精密测量系统<sup>[6-8]</sup>。光栅精密测量系统对环境变化的敏感程度要比激光干涉仪小的多,在环境控制以及测量成本上较激光干涉仪有更大的优势<sup>[9-10]</sup>。

用光栅精密测量系统实现多维度测量的方式目前主要有:(1)用二维光栅代替一维光栅<sup>[11-12]</sup>。(2)采用迈克尔逊干涉仪式的光路结构<sup>[13-14]</sup>。由于二维光栅的制作难度较一维光栅大,光栅的精度和尺寸很难保证。迈克尔逊干涉仪式的光路结构虽然能够测量光栅法线方向的位移,但是由于测量原理的限制,量程受探测器尺寸以及光束直径的限制,测量范围小,最多只有几个毫米,而且系统较为复杂。随后研究者采用利特罗光路结构<sup>[15-17]</sup>,利用一维光栅便可以实现沿光栅矢量和法线方向的二维位移测量,两个维度的测量范围都只受限于光栅的尺寸,大大增加了系统的量程。以上都是光栅精密测量系统扩展位移测量维度的

方式。2009 年 Liu 等人<sup>[18]</sup>在光栅精密测量系统中引入两个四象限二极管探测器 (QPD), 实现了五维自由度测量。由于结构和原理的限制, 该系统的位移测量范围很小, 在实验中沿光栅法线方向的量程只有  $\pm 41 \mu\text{m}$ 。2011 年, Gao 等人<sup>[19]</sup>利用位置灵敏探测器 (PSD) 实现了对光栅三维角度变化的测量。2013 年, 通过结合二维光栅和迈克尔逊干涉仪结构, 该团队提出了六自由度光栅精密测量系统<sup>[20]</sup>。同样由于测量原理和结构的限制, 系统的位移测量范围小, 在实验中, 沿光栅法线方向的量程只有  $1.2 \mu\text{m}$ , 而且系统过于复杂, 降低了系统的可靠性和稳定性。

本文设计了一个具有五维自由度测量能力的光栅精密测量系统。该系统在利特罗式二维光栅位移测量系统的基础上引入角度测量单元实现了位移和角度的同时测量。系统结构简单, 位移测量范围大。文中详细阐述了该系统位移和角度的测量原理, 并通过实验对该系统的性能进行了测试。实验结果表明, 该系统可以实现高精度、高分辨力、大量程的二维位移以及高精度、高分辨力的三维角度测量。

## 2 原 理

### 2.1 读数头的结构

该精密测量系统的读数头包括位移测量单元与角度测量单元。如图 1 所示, 位移测量单元包括一块分束棱镜 BS, 2 块偏振分束棱镜 PBS<sub>1</sub> 和 PBS<sub>2</sub>, 4 片四分之一波片 QW<sub>1</sub>-QW<sub>4</sub>, 2 片衰减片 A<sub>1</sub> 和 A<sub>2</sub>, 2 块平面镜 M<sub>1</sub> 和 M<sub>2</sub>, 2 块半透半反镜 S<sub>1</sub> 和 S<sub>2</sub> 以及两片偏振片 P<sub>1</sub> 和 P<sub>2</sub>。

双频激光器出射的具有一定频差并且偏振方向相互垂直的激光被 BS 分为相同的两束, 分别进入左右两个 PBS。以左侧为例: 激光进入 PBS<sub>1</sub> 后被分为透射光 (P 偏振光) 和反射光 (S 偏振光)。P 偏振光经 QW<sub>1</sub> 变为右旋圆偏振光, 被 S<sub>1</sub> 反射并以利特罗角入射到光栅上, 衍射光线按原路返回, 经过 QW<sub>1</sub> 后变为 S 偏振光并被 PBS<sub>1</sub> 反

射, 通过 P<sub>1</sub> 进入接收器 R<sub>1</sub>。之前的 S 偏振光分别经过 QW<sub>2</sub>、M<sub>1</sub> 和 QW<sub>2</sub> 后变为 P 偏振光, 经偏振分束棱镜透射并通过 P<sub>1</sub> 进入接收器 R<sub>1</sub>。为了使相干的两束光光强接近, 在 QW<sub>2</sub> 和 M<sub>1</sub> 之间加入了衰减片 A<sub>1</sub>。由于 P<sub>1</sub> 的透振方向与光束的振动方向呈  $45^\circ$ , 所以通过 P<sub>1</sub> 的两束光振动方向相互平行, 发生干涉。同样, 右侧部分的两束光也会发生干涉进入接收器 R<sub>2</sub>。

角度测量单元包括两块相同的凸透镜 L<sub>1</sub> 和 L<sub>2</sub> 以及两个位置灵敏探测器 PSD<sub>1</sub> 和 PSD<sub>2</sub>。衍射光经过半透半反镜 S<sub>1</sub> 和 S<sub>2</sub> 后一部分透射进入角度测量单元。PSD 探测器平面放在透镜的焦点处, 激光经过透镜后聚焦在探测器平面, 探测器对聚焦光斑的位置进行实时探测。

### 2.2 位移测量原理

当光栅移动时, 根据光栅多普勒频移原理<sup>[21]</sup>, 两干涉信号会引入相位变化, 分别为:

$$\varphi_1 = \frac{4\pi\sin\theta}{\lambda}\Delta x + \frac{4\pi\cos\theta}{\lambda}\Delta z, \quad (1)$$

$$\varphi_2 = -\frac{4\pi\sin\theta}{\lambda}\Delta x + \frac{4\pi\cos\theta}{\lambda}\Delta z, \quad (2)$$

其中,  $\varphi_1$  和  $\varphi_2$  分别为左右两束测量光束由于光栅运动引入的相位变化,  $\theta$  为激光入射到光栅的利特罗角,  $\lambda$  为激光的波长,  $\Delta x$  为光栅沿光栅矢量方向 ( $x$  方向) 的位移,  $\Delta z$  为光栅沿光栅法线方向 ( $z$  方向) 的位移。

根据公式 (1) 和公式 (2) 以及利特罗入射的光栅方程  $2d\sin\theta = m\lambda$  ( $m = 1, 2, 3 \cdots$ ), 可以计算出光栅沿这两个方向的位移分别为:

$$\Delta x = \frac{d}{4\pi m}(\varphi_1 - \varphi_2), \quad (3)$$

$$\Delta z = (\varphi_1 + \varphi_2) \frac{d}{4\pi m \cot\theta}, \quad (4)$$

其中,  $d$  为光栅的周期。

### 2.3 角度测量原理

当光栅存在角度误差时, 由于入射角的改变, 衍射光线会发生偏转, 从而导致在 PSD 探测器上的光斑位置发生变化。根据几何光学的矩阵分析方法<sup>[22]</sup>可知, 光栅的旋转与 PSD 探测器上光斑位

置的关系如图2所示。

当光栅存在俯仰角变化时,两束衍射光会同时沿光栅刻线方向移动,因此两光斑会沿PSD探测器的 $x$ 轴的相同方向分别移动距离 $x_1$ 和 $x_2$ ,并且 $x_1 = x_2$ ;当光栅存在偏摆误差时,两束衍射光会同时沿光栅矢量方向移动,因此两光斑会沿PSD探测器的 $y$ 轴相同方向分别移动距离 $y_1$ 和 $y_2$ ,并且 $y_1 = y_2$ ;当光栅存在滚转误差时,两光斑会在PSD探测器平面坐标系一、三象限或二、四象限沿相反方向分别移动 $z_1$ 和 $z_2$ ,并且 $|z_1| = |z_2|$ 。由几何关系可以得到光栅的俯仰、偏摆、滚转角度分别为:

$$\theta_x = \frac{x_1 + x_2}{4f}, \quad (5)$$

$$\theta_y = \frac{y_1 + y_2}{4f}, \quad (6)$$

$$\theta_z = \frac{z_1 - z_2}{4f} = \frac{\sqrt{(x_1^2 + y_1^2)} - \sqrt{(x_2^2 + y_2^2)}}{4f}. \quad (7)$$

### 3 实验与测试

为了验证该精密测量系统的性能,搭建了实验平台并进行了一系列的测试实验。测试实验分为角度测试实验和位移测试实验。图3为角度测试实验装置图,波长为632.8 nm的He-Ne双频激光器出射的激光入射到衍射光栅精密测量系统的读数头中,两束光线从读数头中出射,以Littrow角入射到周期为555 nm,尺寸为50 mm × 25 mm × 6 mm的反射光栅上,两衍射光分别经过半透半反射镜后有一部分入射到焦距为400 mm的透镜上,并被透镜汇聚到位于焦面处的两个PSD探测器上,PSD采用的是Newport公司的OBP-U-9H。实验中采用Taylor Hobson公司的精度为0.02"的光电自准直仪DA20检验角度测量的准确性。光栅和两块平面镜都固定在旋转平台上,旋转平台由3块Newport角度位移台组合而成,而且3个平台都安装有该公司的微型压电线性促动器。

图4为位移测试实验装置图。与角度测试实验不同,位移测试实验采用双频激光干涉仪与衍射光栅精密测量系统的位移测量结果进行对比。用Newport公司的精密一维线性位移平台xml210-s代替旋转平台。

图5为静止情况下,衍射光栅精密测量系统对3个方向旋转角度的测量结果。为了方便观察,将俯仰角度和滚转角度的测量结果分别沿 $Y$ 轴正负方向平移2"。从图中可以看出3个角度的测量结果都很稳定,而且振动幅度都很小。高频振动主要是由电子学噪声引起的,其 $3\sigma$ 值分别为0.77"、0.68"和0.72",这同时也可以反映出系统的角度测量分辨力优于1"。

调整微型压电线性促动器,使其最小位移为5step,然后令其做往返运动,由于角度变化较大时会使得位移测量单元无法工作,因此将角度变化范围控制在10"以内。分别得到了衍射光栅精密测量系统和光电自准直仪对俯仰、偏摆、滚转角度的测量结果,如图6~8(彩图见期刊电子版)所示。

3幅图中,带有符号“+”的蓝色实线代表的是衍射光栅精密测量系统对角度的测量结果,红色实线代表的是光电自准直仪的测量结果,黄色实线代表的是二者测量结果之差。从图中可以清楚地看出,两个系统对3个方向的旋转角度的测量结果吻合的都很好,测量结果的差值在零附近波动, $3\sigma$ 值分别为1.18"、1.11"和1.07"。其差值主要是由电子学噪声、环境振动以及未消除干净的余弦误差所引起的。该实验结果证明了衍射光栅精密测量系统能够实现10"内的高精度角度测量,并且具有很好的测量重复性。

图9~11(彩图见期刊电子版)分别为俯仰、偏摆和滚转角度分辨力测试实验结果。调整微型压电线性促动器,使其最小位移为25 step,然后将其与光电自准直仪的测量结果进行对比。图中带“+”的红色实线表示的是衍射光栅精密测量系统的测量结果,蓝色实线代表的是光电自准直仪的测量结果,绿色实线代表的是两系统测量结

果之差。从图中可以看出,压电促动器每走 25 step,角度变化小于  $1''$ 。由于回程误差等因素的影响,测量结果并不是对称的,但是两个系统都可以将该角度的变化检测出来,并且测量结果吻合的很好,二者之差在零附近波动,  $3\sigma$  值分别为  $0.83''$ 、 $0.74''$  和  $0.78''$ 。该实验结果证明衍射光栅精密测量系统的角度测量分辨力优于  $1''$ ,该系统可以进行高精度、高分辨力的角度测量,能够满足精密加工制造的需求。

图 12 ~ 图 15(彩图见期刊电子版)是位移测试实验结果,其中图 12 和 13 分别为在  $x$  方向和  $z$  方向,位移距离为 5 mm 的实验结果。图中带“+”的红色实线表示的是衍射光栅精密测量系统的位移测量结果,蓝色实线表示的是双频激光干涉仪的位移测量结果,小图中的绿色实线表示的是二者位移测量数据的差值。从图 12 中可以看出,对于  $x$  方向上的 5 mm 的位移,衍射光栅精密测量系统和双频激光干涉仪的测量结果吻合的很好,二者之差的  $3\sigma$  为 30.62 nm。从小图中可以看出,两测量结果之差存在一个低频振动。这主要是由光栅的面型、刻线误差以及环境波动引起的。由于光栅面型及刻线的不理想,会在衍射光栅精密测量系统位移测量单元左右两部分中分别引入不同的相位差,从而导致测量结果存在误差。从图 15 中可以看出,对于  $z$  方向上的 5 mm 位移,两个系统的测量结果同样吻合的很好,二者之差的  $3\sigma$  为 20.44 nm。同样,这种情况下的低频振动也主要是由光栅的面型误差、刻线误差以及周围环境变化引起的。由于采用了 Littrow 结构,系统在两个方向上的位移测量量程只受限于光栅的尺寸,而且一维光栅可以做到很长,所以系统很容易实现毫米范围的位移测量,而且随着光栅尺寸的增大,量程还可以增加,远远超出目前采用迈克尔逊结构的多维度测量系统的位移测量范围。

#### 参考文献:

- [1] MALINAUSKAS M, ŽUKAUSKAS A, HASEGAWA S, *et al.*. Ultrafast laser processing of materials: from science to industry [J]. *Light: Science & Applications*, 2016, 5(8): e16133.

图 14 和图 15 分别为  $x$  方向和  $z$  方向的位移分辨力测量结果。图中带“+”的红色实线表示的是衍射光栅精密测量系统的位移测量结果,蓝色实线表示的是双频激光干涉仪的位移测量结果,绿色实线表示的是二者位移测量数据的差值。从两幅图中可以看出,衍射光栅精密测量系统能够测量的小于 4 nm 的位移变化。其与双频激光干涉仪测量数据吻合的较好,二者之差的  $3\sigma$  分别为 1.67 nm 和 2.65 nm。从公式(9)可以看出,  $z$  方向的位移测量值不仅与光栅周期有关,还与入射角度有关,因此受环境影响比  $x$  方向大,所以静止时的位移曲线波动较大,误差较  $x$  方向大一些。

## 4 结 论

本文提出了一种能够同时实现两自由度位移测量和三自由度角度测量的五自由度衍射光栅精密测量系统。该系统解决了现有衍射光栅多维测量系统存在的结构复杂、量程小等问题,具有结构简单,位移量程大,精度和分辨力高的优势。文中详细介绍了系统的基本结构以及测量原理,并针对角度测量和位移测量进行了一系列的测试实验。实验结果表明:该五自由度衍射光栅精密测量系统的三自由度角度测量分辨力优于  $1''$ ,对于  $10''$  的角度变化,其与光电自准直仪测量结果之差的  $3\sigma$  值在  $1''$  左右,对于  $1''$  的角度变化,  $3\sigma$  值在  $0.8''$  左右;两自由度位移测量分辨力优于 4 nm,对于 4 nm 的位移变化,其与双频激光干涉仪的测量结果之差的  $3\sigma$  值在 2 nm 左右,对于 5 mm 的位移变化,  $3\sigma$  值优于 31 nm。该系统结构简单,实用性强,对精密及超精密加工制造领域有着非常重要的意义。

- [2] URNESS A C, MOORE E D, KAMYSIAK K K, et al. . Liquid deposition photolithography for submicrometer resolution three-dimensional index structuring with large throughput [J]. *Light: Science & Applications*, 2013, 2(3) : e56.
- [3] SUGIOKA K, CHENG Y. Ultrafast lasers-reliable tools for advanced materials processing [J]. *Light: Science & Applications*, 2014, 3(4) : e149.
- [4] 敬世美, 张轩宇, 梁居发, 等. 飞秒激光刻写的超短光纤布拉格光栅及其传感特性 [J]. *中国光学*, 2017, 10(4) : 449-454.
- JING SH M, ZHANG X Y, LIANG J F, et al. . Ultrashort fiber Bragg grating written by femtosecond laser and its sensing characteristics [J]. *Chinese Optics*, 2017, 10(4) : 449-454. ( in Chinese)
- [5] 陈宝刚, 明名, 吕天宇. 大口径球面反射镜曲率半径的精确测量 [J]. *中国光学*, 2014, 7(1) : 163-168.
- CHEN B G, MING M, LV T Y. Precise measurement of curvature radius for spherical mirror with large aperture [J]. *Chinese Optics*, 2014, 7(1) : 163-168. ( in Chinese)
- [6] LOU Y T, YAN L P, CHEN B Y, et al. . Laser homodyne straightness interferometer with simultaneous measurement of six degrees of freedom motion errors for precision linear stage metrology [J]. *Optics Express*, 2017, 25(6) : 6805-6821.
- [7] ZHANG E ZH, CHEN B Y, ZHENG H, et al. . Laser heterodyne interferometer with rotational error compensation for precision displacement measurement [J]. *Optics Express*, 2018, 26(1) : 90-98.
- [8] 吕强, 李文昊, 巴音贺希格, 等. 基于衍射光栅的干涉式精密位移测量系统 [J]. *中国光学*, 2017, 10(1) : 39-50.
- LV Q, LI W H, BAYANHESHIG, et al. . Interferometric precision displacement measurement system based on diffraction grating [J]. *Chinese Optics*, 2017, 10(1) : 39-50. ( in Chinese)
- [9] ESTLER W T. High-accuracy displacement interferometry refin air [J]. *Applied Optics*, 1985, 24(6) : 808-815.
- [10] GERASIMOV F M. Use of diffraction gratings for controlling a ruling engine [J]. *Applied Optics*, 1967, 6(11) : 1861-1865.
- [11] HSIEH H L, CHEN J C, LERONDEL G, et al. . Two-dimensional displacement measurement by quasi-common-optical-path heterodyne grating interferometer [J]. *Optics Express*, 2011, 19(10) : 9770-9782.
- [12] CHUNG Y CH, FAN K C, LEE B C. Development of a novel planar encoder for 2D displacement measurement in nanometer resolution and accuracy [C]. *Proceedings of the 2011 9th World Congress on Intelligent Control and Automation*, IEEE, 2011: 449-453.
- [13] GAO W, KIMURA A. A three-axis displacement sensor with nanometric resolution [J]. *CIRP Annals*, 2007, 56(1) : 529-532.
- [14] KIMURA A, GAO W, KIM W, et al. . A sub-nanometric three-axis surface encoder with short-period planar gratings for stage motion measurement [J]. *Precision Engineering*, 2012, 36(4) : 576-585.
- [15] LU Y C, WEI CH L, JIA W, et al. . Two-degree-freedom displacement measurement based on a short period grating in symmetric Littrow configuration [J]. *Optics Communications*, 2016, 380: 382-386.
- [16] ŠIAUDINYTĖ L, MOLNAR G, KÖNING R, et al. . Multi-dimensional grating interferometer based on fibre-fed measurement heads arranged in Littrow configuration [J]. *Measurement Science and Technology*, 2018, 29(5) : 054007.
- [17] LV Q, LIU ZH W, WANG W, et al. . Simple and compact grating-based heterodyne interferometer with the Littrow configuration for high-accuracy and long-range measurement of two-dimensional displacement [J]. *Applied Optics*, 2018, 57(31) : 9455-9463.
- [18] LIU C H, HUANG H L, LEE H W. Five-degrees-of-freedom diffractive laser encoder [J]. *Applied Optics*, 2009, 48(14) : 2767-2777.
- [19] GAO W, SAITO Y, MUTO H, et al. . A three-axis autocollimator for detection of angular error motions of a precision stage [J]. *CIRP Annals*, 2011, 60(1) : 515-518.
- [20] LI X H, GAO W, MUTO H, et al. . A six-degree-of-freedom surface encoder for precision positioning of a planar motion

- stage [J]. *Precision Engineering*, 2013, 37(3): 771-781.
- [21] TEIMEL A. Technology and applications of grating interferometers in high-precision measurement [J]. *Precision Engineering*, 1992, 14(3): 147-154.
- [22] 周炳琨, 高以智, 陈倜嵘, 等. 激光原理 [M]. 6 版. 北京: 国防工业出版社, 2009.
- ZHOU B K, GAO Y ZH, CHEN T R, *et al.*. *Laser Principle* [M]. 6th ed. Beijing: National Defense Industry Press, 2009. (in Chinese)

#### 作者简介:



LV Qiang(1992—), Male, from Dezhou, Shandong, Ph.D. and is mainly engaged in diffraction grating and precision measurement. E-mail: lq\_0119@126.com

吕强(1992—),男,山东德州人,博士研究生,2014 年于山东师范大学获得学士学位,2019 年于中国科学院长春光学精密机械与物理研究所获得博士学位,主要从事衍射光栅及精密测量等方面的研究。E-mail: lq\_0119@126.com



LI Wen-hao (1980—), male, from Chifeng, Inner Mongolia, professor, and is mainly engaged in optical diffractive element, optical communication devices, high precision displacement measurement. E-mail: liwh@comp.ac.cn

李文昊(1980—),男,内蒙古赤峰人,博士,研究员,2002 年于陕西科技大学获得学士学位,2008 年于中国科学院长春光学精密机械与物理研究所获得博士学位,主要从事平面、凹面全息光栅的理论设计及制作工艺,光谱仪器、精密位移测量等方面的研究。E-mail: liwh@ciomp.ac.cn